Available online at www.sciencedirect.com
SCIENCE DIRECT®
Journal of Molecular Catalysis A: Chemical 212 (2004) 229–236
JOURNAL OF MOLECULAR CATALYSIS A: CHEMICAL
www.elsevier.com/locate/molcata

Redox properties of Keggin-type heteropolyacid (HPA) catalysts: effect of counter-cation, heteroatom, and polyatom substitution

In K. Song [a,*], Mark A. Barteau [b]

[a] *Department of Environmental & Applied Chemical Engineering, Kangnung National University, Kangnung 210-702, South Korea*
[b] *Center for Catalytic Science and Technology, Department of Chemical Engineering, University of Delaware, Newark, DE 19716, USA*

Received 17 June 2003; received in revised form 28 August 2003; accepted 26 October 2003

Abstract

Redox properties of Keggin-type heteropolyacid (HPA) catalysts were determined with the aim of providing a reduction potential database of these compounds. Cation-exchanged, polyatom-substituted, and heteroatom-substituted HPAs were examined to investigate the effects of different substitutions. Reduction potentials of HPA samples were determined by electrochemical methods. The reduction potentials of HPA catalysts could be correlated with the electronegativity of the substituted atoms. Substitution of more electronegative atoms for counter-cations or for the central heteroatom increased reduction potentials of the HPAs. However, substitution of more electronegative metals into the Keggin framework decreased reduction potentials. This work demonstrates how one can estimate or predict reduction potentials of Keggin-type HPA catalysts. A map of reduction potentials of HPA catalysts was established to provide a design basis in searching for catalytic oxidation processes using HPAs.

Keywords: Heteropolyacid (HPA) catalyst; Reduction potential; Cyclovoltametry; Oxidation catalyst; Redox properties

1. Introduction

Heteropolyacids (HPAs) are early transition metal oxygen anion clusters that exhibit a wide range of molecular sizes, compositions, and architectures [1]. Among various HPA structural classes, the Keggin-type [2] HPAs have been widely employed as catalysts in homogeneous and heterogeneous systems for acid–base and oxidation reactions [3–8]. One of the great advantages of HPA catalysts is their great thermal stability [9]. This stability makes HPAs good candidates for catalytic and sensor applications which may require harsh environments.

The catalytic redox activity of HPAs has attracted much attention [10–12]. HPAs have been investigated as oxidation catalysts to make useful chemicals directly from hydrocarbon raw materials, including oxidation of propane to acrylic acid [13–15], and oxidation of isobutane to methacrolein and methacrylic acid [16,17]. Several theoretical and instrumental methods have been employed to determine the reduction potential (oxidizing power) of HPAs. For example, quantum chemical studies have attempted to elucidate the reduction potentials of selected HPAs [18,19]. Absorption edge positions in the UV-Vis spectra of HPAs have been suggested to reflect the reduction potential of HPAs [20]. Reduction trends of cation-exchanged $RPMo_{12}O_{40}$ (M = H_3, $Cu_{3/2}$, $Co_{3/2}$, $Ba_{3/2}$, etc.) HPAs in solid form have also been reported [21]. Another promising approach is to determine the reduction potential of HPA catalysts from negative differential resistance (NDR) peak voltages in tunneling spectra measured with a scanning tunneling microscope (STM) [22–28].

However, the most conventional technique to determine the reduction potentials of HPA catalysts is electrochemical. Electrochemical reduction potential data for several series of HPAs in solutions have been reported. These examples include heteroatom-substituted $H_nXMo_{12}O_{40}$ (X = P, As, Si, Ge) HPAs [18], heteroatom-substituted $H_nXW_{12}O_{40}$ (X = P, Si, Co, Fe, B) HPAs [29–32], heteroatom(P, Si)- and polyatom(W, Mo)-substituted HPAs [33], polyatom(Mo, V)-substituted HPAs [30,34], and various HPA samples under different measurement conditions [35]. Presently, however, an extensive reduction potential database of HPAs

* Corresponding author. Tel.: +82-33-640-2404; fax: +82-33-640-2244.
E-mail address: inksong@kangnung.ac.kr (I.K. Song).

1381-1169/$ – see front matter © 2003 Elsevier B.V. All rights reserved.
doi:10.1016/j.molcata.2003.10.040

measured by a consistent method under consistent conditions is not available. In general, the reduction potential of an HPA sample depends on the identity/composition of electrolyte solution (pH), the identity of the electrodes, etc. [31,36]. Therefore, direct comparison of reduction potentials of HPA catalysts from literature reports is not a simple task [32].

The aim of this work is to provide an extensive database of reduction potentials of HPA catalysts for the direct comparison of HPA reduction potentials. Therefore, extensive and detailed analyses of reduction–oxidation mechanisms of HPA samples were not included in this work. Keggin-type HPAs with different counter-cation, polyatom, and heteroatom substitutions were examined in a systematic way in this study. The measured reduction potentials of HPA samples were correlated with the electronegativities of the substituted atoms. This work shows how one can estimate or predict reduction potentials of Keggin-type HPA catalysts. The experiments were designed to be as simple as possible in order to avoid complexity and to maintain consistent measurement conditions.

Fig. 1 shows the molecular structure of the pseudo-spherical (T_d symmetry) Keggin-type $[PMo_{12}O_{40}]^{3-}$ heteropolyanion constructed from X-ray crystallography data [37,38]. The molecular structure of $[PMo_{12}O_{40}]^{3-}$ consists of a heteroatom, P, at the center of the anion cluster, tetrahedrally coordinated to four oxygen atoms. This tetrahedron is surrounded by 12 MoO_6 octahedra. The van der Waals diameter along the three-fold axis of symmetry is 11.97 Å. It is known that the redox properties of HPAs can be tuned by changing the identity of charge-compensating counter-cations, heteroatoms, and framework metal atoms (polyatoms) [3,10,11,31].

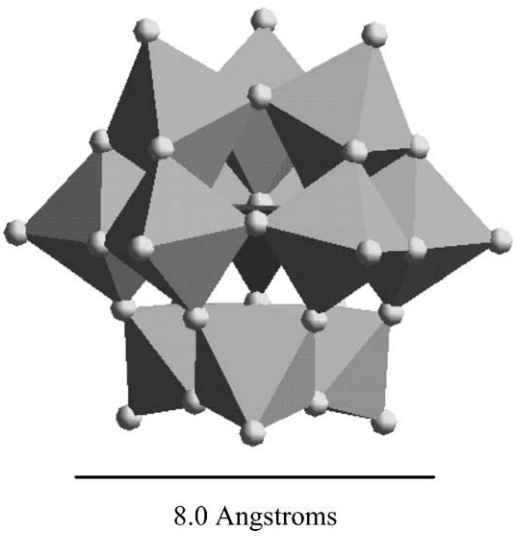

Fig. 1. Polyhedral representation of the molecular structure of the pseudo-spherical Keggin-type $[PMo_{12}O_{40}]^{3-}$ heteropolyanion (primary structure).

2. Experimental

2.1. Materials

The following series of HPAs were investigated to explore their reduction potentials: cation-exchanged $RPMo_{12}O_{40}$ (R = H_3, $Zn_{3/2}$, $Co_{3/2}$, $Cu_{3/2}$, Bi_1), heteroatom-substituted $H_nXW_{12}O_{40}$ (X = P, Si, B, Co) and $H_nXMo_{12}O_{40}$ (X = P, As, Si), polyatom-substituted $H_nPW_{11}M_1O_{40}$ (M = W, Mo, V), $H_3PMo_xW_{12-x}O_{40}$ ($x = 0, 3, 6, 9, 12$), $H_{3+x}PMo_{12-x}V_xO_{40}$ ($x = 0, 1, 2, 3$), and $H_{3+x}PW_{12-x}V_xO_{40}$ ($x = 0, 1, 2, 3$) HPAs. Commercially available $H_3PMo_xW_{12-x}O_{40}$ ($x = 0, 3, 6, 9, 12$), $H_{3+x}PMo_{12-x}V_xO_{40}$ ($x = 0, 1, 2, 3$), $H_{3+x}PW_{12-x}V_xO_{40}$ ($x = 0, 1, 2, 3$), $H_4SiMo_{12}O_{40}$, and $H_4SiW_{12}O_{40}$ samples were purchased from Aldrich Chemical Co. and Nippon Inorganic Color and Chemical Co. $H_5BW_{12}O_{40}$ and $H_6CoW_{12}O_{40}$ were kindly provided by Prof. Craig L. Hill at Emory University. $H_3AsMo_{12}O_{40}$ from Sunoco was provided by Dr. James E. Lyons. Cation-exchanged HPAs were prepared by replacing all protons of $H_3PMo_{12}O_{40}$ with metal atoms, according to published methods [21].

2.2. Measurement of reduction potential

Reduction potentials of HPA samples were measured electrochemically. The electrochemical measurements were made with a Potentiostat/Galvanostat Model 263A (Perkin-Elmer) and a computer-controlled cyclovoltametry system. The working electrode was solid Pt with an electrode area of 1 cm^2. Pt wire and Ag/AgCl (KCl saturated) were used as the counter electrode and the reference electrode, respectively. To obtain cyclovoltagrams, 1 mM of each HPA sample dissolved in 0.5 M Na_2SO_4 aqueous electrolyte solution (10 ml) was prepared. The samples were purged with helium (50 cm^3/min) for 2 min. The samples were then maintained for 1 min for stabilization prior to measurement of cyclovoltagrams. Cyclovoltagrams were obtained at the scan rate of 10 mV/s.

3. Results and discussion

3.1. Stabilities and reduction potentials of HPAs

Many attempts have been made to measure the reduction potentials of HPA samples, as described previously [18,29–36]. A survey of the literature shows that many kinds of electrolyte solutions have been used for electrochemical measurements of HPA reduction potentials. Examples include H_2SO_4 [29], dioxane-H_2SO_4 [33], $HClO_4$ [39], CH_3CN-HCl [40], and Na_2SO_4 solutions [29,41]. The identity and composition of the electrolyte solution affects the pH of the HPA solution. In our experiments, 0.5 M Na_2SO_4 aqueous electrolyte solution was used. No additional physical and chemical treatments were done to the samples in

order to carry out the experiments as simply as possible and to keep the experimental conditions as similar as possible. The pH values of HPA solution samples examined in this work were in the range of ca. 3.0–3.3 (pure acids-HPA salts). The stabilities of HPAs in solution at a given pH are also important to consider in comparing reduction potential measurements for different HPA catalysts.

The stabilities of HPA samples at various pH values have been studied by a number of researchers [42–47], and include studies of the decomposition of 12-tungstosilicate [42] and 12-molybdophosphate [43–45]. A study of the stability of $H_3PMo_{12}O_{40}$, $H_3PW_{12}O_{40}$, $H_4SiMo_{12}O_{40}$, and $H_4SiW_{12}O_{40}$ HPA samples in aqueous solution at varying pH was carried out by McGarvey and Moffat [47]. They reported that $H_3PMo_{12}O_{40}$, $H_3PW_{12}O_{40}$, $H_4SiMo_{12}O_{40}$, and $H_4SiW_{12}O_{40}$ HPA solution samples were relatively stable at low pH, but they were completely decomposed at higher pH values of 4.0, 5.2, 7.0, and 11.0, respectively. The stability was reported to be in the order $H_4SiW_{12}O_{40}$ > $H_3PW_{12}O_{40}$ > $H_4SiMo_{12}O_{40}$ > $H_3PMo_{12}O_{40}$. That work [47] also showed that the extent of HPA decomposition was time-dependent. Experimental data in the same report showed the following results for the extreme experimental cases: 2% of $H_4SiW_{12}O_{40}$ decomposed at pH 4.7 after 1 week; likewise 9% of $H_3PW_{12}O_{40}$ at pH 4.4 after 1 week, 50% of $H_4SiMo_{12}O_{40}$ at pH 4.2 after 24 h, and 100% of $H_3PMo_{12}O_{40}$ at pH 4.0 after 24 h were decomposed. Extrapolation of the results for $H_4SiW_{12}O_{40}$, $H_3PW_{12}O_{40}$, and $H_4SiMo_{12}O_{40}$ HPA samples suggested that the fraction of these HPA samples that would be decomposed at pH 3.0 after 24 h would be at most ca. 5%. In our experiments, each measurement, including the preparation of HPA solution sample was completed within 10 min. Therefore, it is inferred that these samples should be stable at least during our experimental measurements. Solution chemistry also showed that polyatom-substituted $[PMo_9V_3O_{40}]^{6-}$ and $[PMo_6V_6O_{40}]^{9-}$ HPA samples were stable at the pH 2.5–5.5 [48].

The pH value of the $H_3PMo_{12}O_{40}$ solution sample examined in this work was 3.1. Previous investigations [44,46] showed that $H_3PMo_{12}O_{40}$ was stable in an aqueous solution at pH less than 1.5. As the pH increased with the presence of $[OH]^-$, this HPA underwent alkaline hydrolysis in dilute solution ($<10^{-3}$ mol/l) [44]. That work also revealed that $H_6P_2Mo_{18}O_{62}$ was formed in aqueous solution at pH values less than 3.0, but the rate was very slow and it took about 1 month for the full formation of this species. The stability of HPAs including $H_3PMo_{12}O_{40}$ increases in organic media [40,45]. It is known from conductivity studies that HPAs such as $H_3PMo_{12}O_{40}$ are stable toward solvolysis in ethanol, acetone, and acetic acid at concentrations as low as 10^{-5}–10^{-6} mol/l [49], and equilibration rates between various species are decreased by the addition of an organic solvent [40,45].

The dependence of the stability of the $H_3PMo_{12}O_{40}$ solution sample on pH was investigated by IR analyses in a previous work [46]. The characteristic IR bands of stable $[PMo_{12}O_{40}]^{3-}$ appear at 1065, 960, 870, and 785 cm^{-1}, which are attributed to P–O, Mo=O, interoctahedral Mo–O–Mo, and intraoctahedral Mo–O–Mo bands, respectively. That work [46] reported that these bands were maintained with no changes up to pH value of 1.5, but the band at 1065 cm^{-1} split into two bands at pH 2.0, representing the existence of $[PMo_{11}O_{39}]^{7-}$ species. It was also reported by the same authors that bands at ≈965, 895, and 565 cm^{-1} representing $[P_2Mo_5O_{23}]^{6-}$ species were observed at pH 5.0.

In order to ensure the stability of the $H_3PMo_{12}O_{40}$, HPA solution sample during the time period of our experimental measurements (less than 10 min for each run), IR measurements were taken (JASCO, FT-IR/460 Plus). Many attempts were made to resolve an IR spectrum of $H_3PMo_{12}O_{40}$ HPA (1 mM) dissolved in 0.5 M Na_2SO_4 aqueous solution (pH 3.1). However, it was not a simple task to obtain an IR spectrum of the solution sample because of the strong absorbance by the hydroxyl group of water. Instead we examined solid $H_3PMo_{12}O_{40}$ samples, formed by evaporating $H_3PMo_{12}O_{40}$ aqueous solutions with different pH. The aqueous $H_3PMo_{12}O_{40}$ solutions with different pH (with different $H_3PMo_{12}O_{40}$ concentration) were prepared and maintained for 10 min, and then they were dried as quickly as possible to yield solid samples. It took ca. 20 min from $H_3PMo_{12}O_{40}$ dissolution to IR measurement. Fig. 2 shows the IR spectra of solid $H_3PMo_{12}O_{40}$ samples that were recrystallized from aqueous solutions with different pH. Fig. 2 shows that pure solid $H_3PMo_{12}O_{40}$ exhibits the character-

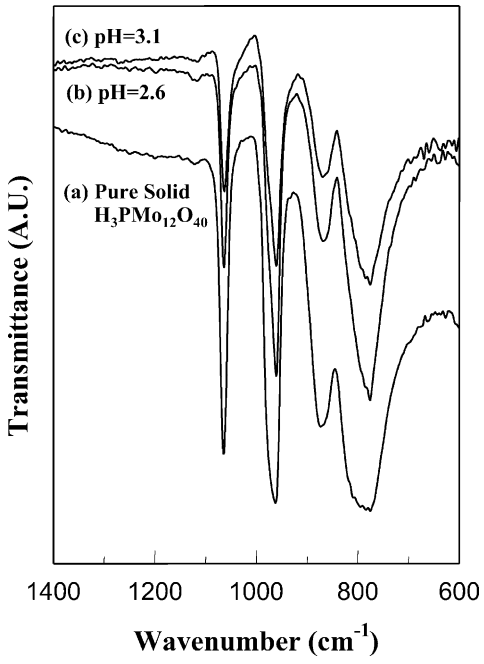

Fig. 2. IR spectra of (a) pure solid $H_3PMo_{12}O_{40}$, (b) $H_3PMo_{12}O_{40}$ recrystallized from aqueous solution of pH 2.6, and (c) $H_3PMo_{12}O_{40}$ recrystallized from aqueous solution of pH 3.1.

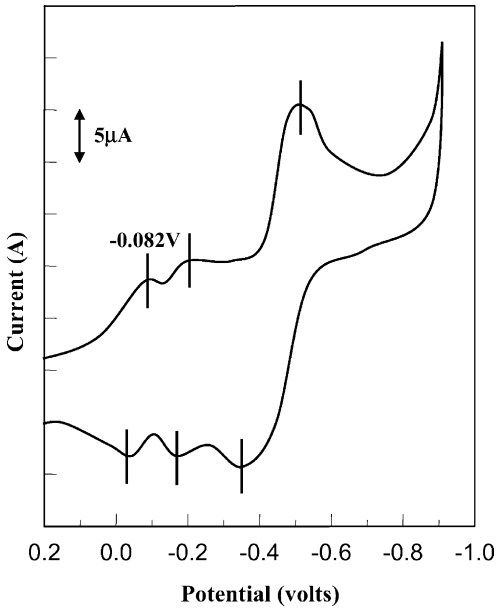

Fig. 3. A cyclovoltagram of 1 mM $H_3PMo_{12}O_{40}$ sample dissolved in 0.5 M Na_2SO_4 aqueous electrolyte solution (10 ml).

istic IR bands of $[PMo_{12}O_{40}]^{3-}$ appearing at 1065, 960, 870, and 782 cm^{-1}, in good agreement with the previous result [46]. Importantly, the solid samples recrystallized from aqueous solutions with different pH show four characteristic IR bands at the same positions as those of pure solid $H_3PMo_{12}O_{40}$, without P–O band splitting. These results indicate either that the $H_3PMo_{12}O_{40}$ HPA in solution is stable at the pH levels employed for the brief duration of our experiments, or that any transformation is readily reversible on the same time scale. Thus, the reduction potentials reported here represent those of the HPAs and potentially any structures in equilibrium with them. In the absence of any indications of the existence of the latter, it is therefore appropriate to consider these results as representative of the chemical properties of intact HPAs.

Fig. 3 shows the typical cyclovoltagram of 1 mM $H_3PMo_{12}O_{40}$ sample dissolved in 0.5 M Na_2SO_4 aqueous electrolyte solution (10 ml). Reduction waves were observed with peak potentials at −0.082, −0.215, and −0.501 V. The anodic peaks were occurred at −0.025, −0.171, and −0.353 V in the reverse scan. According to the literature [9], Keggin-type HPAs exhibit 'mono-oxo'-type reduction–oxidation ability. It is known that cyclovoltagrams of Keggin-type HPAs show a sequence of reversible one- or two-electron reductions which yield deeply colored heteroply blues [40,50]. Thermodynamic and kinetic aspects of reduction–oxidation mechanisms of various HPAs are also available [51]. An electrochemical investigation [29] of the reduction potentials of $[XW_{12}O_{40}]^{n-}$ (X = P, Si, Fe, Co) HPA samples dissolved in H_2SO_4 or Na_2SO_4 electrolyte solution revealed that the half-wave one-electron reduction potentials of $[PW_{12}O_{40}]^{3-}$, $[SiW_{12}O_{40}]^{4-}$, and $[FeW_{12}O_{40}]^{5-}$ were unaltered and pH-independent. That work [29] also showed that the reduction wave of the $[CoW_{12}O_{40}]^{6-}$ sample gradually split into two waves with increasing pH. However, the first half-wave one-electron reduction potential of $[CoW_{12}O_{40}]^{6-}$ HPA was pH-independent up to the pH value of 4.9. Another electrochemical study of the $[AlW_{12}O_{40}]^{5-}$ HPA samples, carried out by Hill and co-workers within a pH range of 1.5–4.0, revealed that the first electron reduction potentials (also half-wave one-electron reduction potentials) were almost constant, whereas the second and third reduction peak potentials decreased with increasing pH [52]. In our study, therefore, the first electron reduction potential was taken as the representative reduction potential of the HPA. The first electron reduction potential of $H_3PMo_{12}O_{40}$ was thus −0.082 V.

3.2. Effect of counter-cation substitution

Previous work [21] has shown that characteristics related to reduction potential, such as the activation barrier for reduction, decreased when the protons of the $H_3PMo_{12}O_{40}$ were replaced by more electronegative cations such as Cu^{2+} in the solid. Conversely, the reduction potential decreased (barrier to reduction increased) when the protons were replaced by less electronegative cations such as Cs^+. This indicates that the electronegativity of the counter-cations is very important in determining the reduction potentials of HPAs. In other words, reduction potentials of cation-exchanged HPAs can be controlled by the electronegativity of the counter-cation.

A comprehensive trend for reduction potentials of cation-exchanged HPAs with respect to counter-cation electronegativities was established by investigating a set of cation-exchanged $RPMo_{12}O_{40}$ (R = H_3, $Zn_{3/2}$, $Co_{3/2}$, $Cu_{3/2}$, Bi_1) HPAs, covering a wide range of counter-cation Tanaka electronegativities [53]. All these HPA salts were soluble in the Na_2SO_4 electrolyte solution. Fig. 4 shows

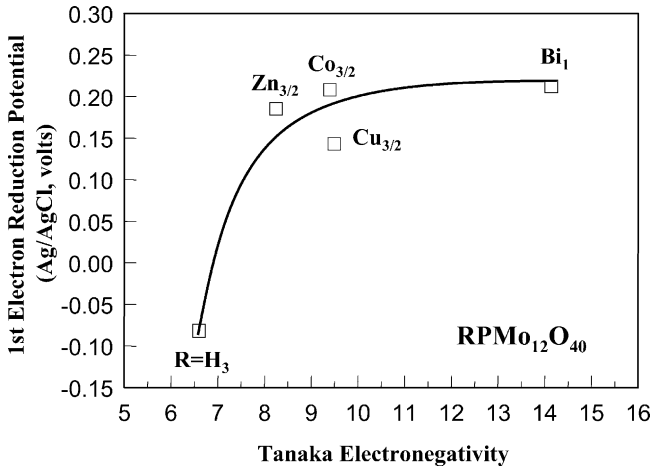

Fig. 4. Correlation between reduction potentials of cation-exchanged $RPMo_{12}O_{40}$ (R = H_3, $Zn_{3/2}$, $Co_{3/2}$, $Cu_{3/2}$, Bi_1) HPAs and Tanaka electronegativities of the counter-cation.

the reduction potentials of cation-exchanged HPAs plotted with respect to the Tanaka electronegativities [53] of the counter-cations (The Tanaka electronegativity takes into account the electron-donating and -accepting ability of the atom). The reduction potentials of cation-exchanged HPAs measured in solution increased with increasing electronegativity of the counter-cation. In other words, the HPA salts with more electronegative counter-cations had higher reduction potentials. This trend is in agreement with results obtained for cation-exchanged HPA samples in solids [21].

The variation of reduction potentials of cation-exchanged HPA samples with the same heteropolyanion is not surprising. A previous work [36] investigating reduction potentials of alkali salts (Li, Na, K) of $[XVW_{11}O_{40}]^{n-}$ (X = P, Si, Al) HPA samples measured electrochemically also showed variations of reduction potentials of HPA salts depending on the identity of counter-cation, even for the HPA samples with the same heteropolyanion. The reduction potentials of these HPA salts were also observed to increase with decreasing Tanaka electronegativity of the alkali metal ions.

3.3. Effect of heteroatom substitution

Fig. 5(a) shows the correlation between reduction potentials of heteroatom-substituted $H_nXW_{12}O_{40}$ (X = P, Si, B, Co) HPAs and Tanaka electronegativities of the heteroatoms. As shown in Fig. 5(a), the reduction potentials of $H_nXW_{12}O_{40}$ (X = P, Si, B, Co) samples increased with increases in the electronegativity of the heteroatom. The trend of reduction potentials of $H_nXW_{12}O_{40}$ (X = P, Si, B, Co) HPAs shown in Fig. 5(a) was in good agreement with the previous results [30–32] (closed symbols, shown for comparison). A previous report [29] also showed that half-wave one-electron reduction potentials of $[XW_{12}O_{40}]^{n-}$ HPAs were in the order $[PW_{12}O_{40}]^{3-}$ (−0.023 V) > $[SiW_{12}O_{40}]^{4-}$ (−0.187 V) > $[CoW_{12}O_{40}]^{6-}$ (−0.510 V), in good agreement with the results in Fig. 5(a). Fig. 5(b) shows the correlation between reduction potentials of heteroatom-substituted $H_nXMo_{12}O_{40}$ (X = P, As, Si) HPAs and Tanaka electronegativities of the heteroatoms. This figure also shows that the reduction potentials of $H_nXMo_{12}O_{40}$ (X = P, As, Si) samples increased with increases in the electronegativity of the heteroatom. Furthermore, the trend of reduction potentials of $H_nXMo_{12}O_{40}$ (X = P, As, Si) HPAs was also in good agreement with previous results [18] (closed symbols, shown for comparison). However, the quantitative differences between reduction potentials of different HPAs were not directly comparable because of the different measurement conditions between this and previous studies.

A previous study [18] investigating a set of heteroatom-substituted $H_nXMo_{12}O_{40}$ (X = As, P, Ge, Si) HPAs demonstrated that reduction potentials of the HPAs (determined by polarographic methods) increased in the order Si (0.475 V) < Ge (0.492 V) < P (0.518 V) < As (0.526 V). According to quantum chemical calculations for $H_3PMo_{12}O_{40}$, the lowest unoccupied molecular orbital (LUMO) is a mixture of 4d-orbitals of Mo and 2p-orbitals of the bridging oxygen atoms, while the highest occupied molecular orbital (HOMO) is mostly composed of 2p-orbitals of bridging oxygens [54]. Theoretical calculations for $H_nXMo_{12}O_{40}$ (X = As, P, Ge, Si) HPAs revealed that the LUMO is responsible for reduction of HPAs [18]. The calculated energy values of the LUMO for $H_nXMo_{12}O_{40}$ (X = As, P, Ge, Si) HPAs followed the order Si > Ge > P > As, suggesting that $H_3AsMo_{12}O_{40}$ is the most reducible and $H_4SiMo_{12}O_{40}$ is the least reducible [18]. The order of Tanaka electronegativities of the heteroatoms in this HPA series gives the sequence Si < Ge < As ≈ P. These results are consistent with the results in Fig. 5(b). The reduction potential dependence of the $H_nXMo_{12}O_{40}$ (X = As, P, Si) HPAs on the electronegativities of the heteroatoms (Fig. 5(b)) is consistent with that observed for $H_nXW_{12}O_{40}$ (X = P, Si, B, Co) HPAs (Fig. 5(a)).

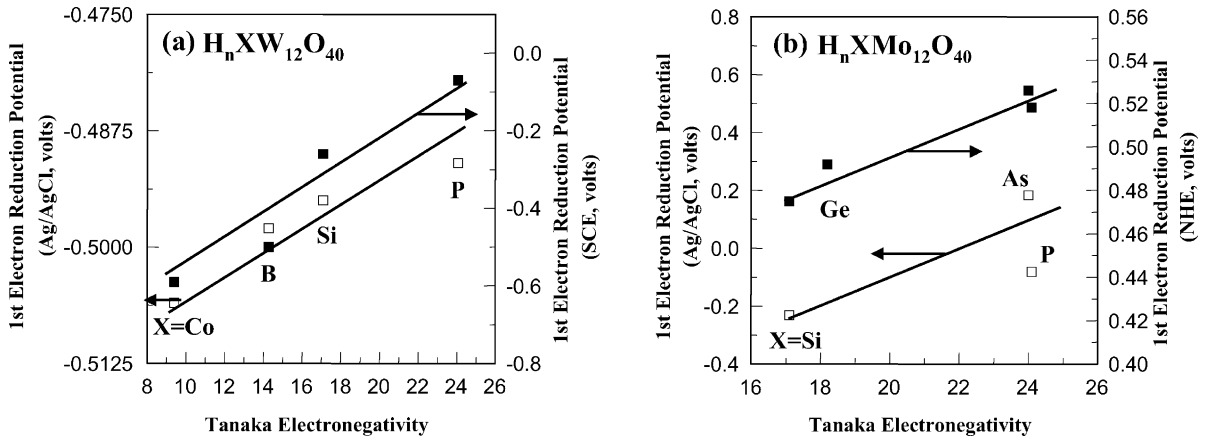

Fig. 5. Correlation between reduction potentials of heteroatom-substituted HPAs and Tanaka electronegativities of the heteroatom, established for families of (a) $H_nXW_{12}O_{40}$ (X = P, Si, B, Co) and (b) $H_nXMo_{12}O_{40}$ (X = P, As, Si) HPAs. Closed symbols represent reduction potentials of HPA samples taken from the literature ([30–32] for Fig. 5(a) and [18] for Fig. 5(b)).

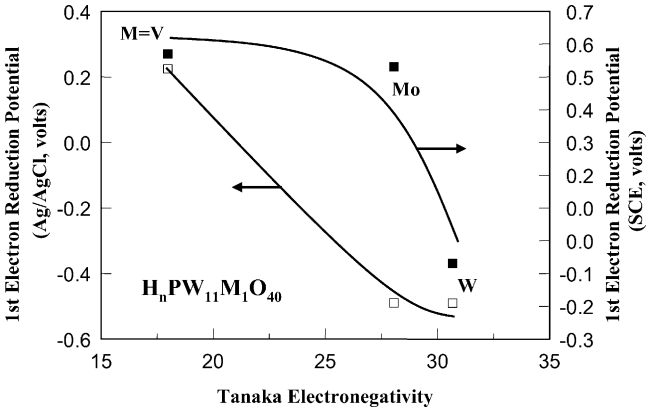

Fig. 6. Correlation between reduction potentials of polyatom-substituted $H_nPW_{11}M_1O_{40}$ (M = W, Mo, V) HPAs and Tanaka electronegativities of the polyatom. Closed symbols represent reduction potentials of HPA samples taken from the literature [30,31].

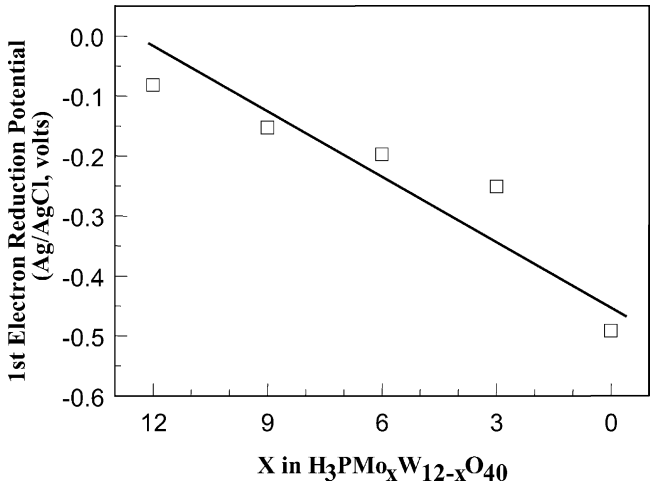

Fig. 7. Reduction potentials of polyatom-substituted $H_3PMo_xW_{12-x}O_{40}$ ($x = 0, 3, 6, 9, 12$) HPAs plotted as a function of the number of molybdenum atoms substitution.

Interestingly, Fig. 5(a) and (b) clearly show that the reduction potential dependencies on the electronegativity of heteroatoms exhibit the same trends as those observed for cation-exchanged HPA samples (Fig. 4). Taken together, these results suggest that electron-donating and electron-accepting ability of atoms not located in the metal–oxygen framework of the Keggin ion have a similar effect on the reduction potential, whether these atoms are the heteroatoms in the Keggin interior, or counter-cations on the exterior.

3.4. Effect of polyatom substitution

Fig. 6 shows the correlation between reduction potentials of polyatom-substituted $H_nPW_{11}M_1O_{40}$ (M = W, Mo, V) HPAs and the Tanaka electronegativities of the polyatoms. The overall trend of reduction potentials of $H_nPW_{11}M_1O_{40}$ (M = W, Mo, V) HPAs was in good agreement with literature results [30,31] (shown as closed symbols). Again, quantitative comparisons between these results are not possible because of the different measurement conditions. Fig. 6 clearly shows that the reduction potentials of $H_nPW_{11}M_1O_{40}$ (M = W, Mo, V) samples decrease with increasing electronegativity of the polyatom. What is surprising about the results in Fig. 6 is that the trend of reduction potential of polyatom-substituted HPAs with respect to polyatom electronegativity is the opposite of those observed for the cation-exchanged HPAs (Fig. 4) and for heteroatom-substituted HPAs (Fig. 5).

Fig. 7 shows the reduction potential of polyatom-substituted $H_3PMo_xW_{12-x}O_{40}$ ($x = 0$–12) HPAs plotted with respect to the Mo content. The reduction potentials of these samples increased in a monotonic fashion with increasing Mo content. When considering that molybdenum is less electronegative than tungsten, the dependence of reduction potential on the polyatom electronegativity observed for $H_3PMo_xW_{12-x}O_{40}$ ($x = 0$–12) HPAs shows the same trend as that shown in Fig. 6.

The effect of framework vanadium substitution on the reduction potential of HPAs is somewhat complicated. As shown in Fig. 8(a) for a series of $H_{3+x}PMo_{12-x}V_xO_{40}$ ($x = 0$–3) samples, it was observed that reduction potential of these HPAs did not vary monotonically with the number of vanadium ions substituted (note that vanadium is less electronegative than molybdenum). Instead, the reduction potential of $H_{3+x}PMo_{12-x}V_xO_{40}$ ($x = 0$–3) samples shows a maximum when $x = 1$. Fig. 8(b) also shows the reduction potential of $H_{3+x}PW_{12-x}V_xO_{40}$ ($x = 0$–3) samples as a function of vanadium substitution. As observed for a series of $H_{3+x}PMo_{12-x}V_xO_{40}$ ($x = 0$–3) samples, the reduction potential of $H_{3+x}PW_{12-x}V_xO_{40}$ ($x = 0$–3) samples did not vary monotonically with the number of vanadium substitution, and the reduction potential of these HPAs also showed a maximum when $x = 1$. Previous work [34,55] reported that the reduction potential of $H_{3+x}PMo_{12-x}V_xO_{40}$ ($x = 0$–3) HPAs exhibited a maximum when $x = 2$, while other work [56] reported that the reduction potential of these HPA samples showed a maximum when $x = 1$. As mentioned earlier, the reduction potential of an HPA depends on measurement conditions such as in solutions or in solids, the type/composition of electrolytes (pH), the type of electrodes, etc. Therefore, the above differences may be due to different measurement conditions of the HPA reduction potentials.

The effect of vanadium substitution was elucidated by a molecular orbital study on the $H_nPM_{12-x}V_xO_{40}$ (M = Mo, W; $x = 0$–3) HPAs [19]. It was reported that the energy gap between the HOMO and the LUMO was consistent with reduction potential of the HPAs; more reducible HPAs showed the smaller energy gaps. That work also showed that the HOMO for all HPAs consists primarily of nonbonding p-orbitals on the oxygens of the HPAs, while the LUMO consists of an antibonding combination of d-orbitals on the

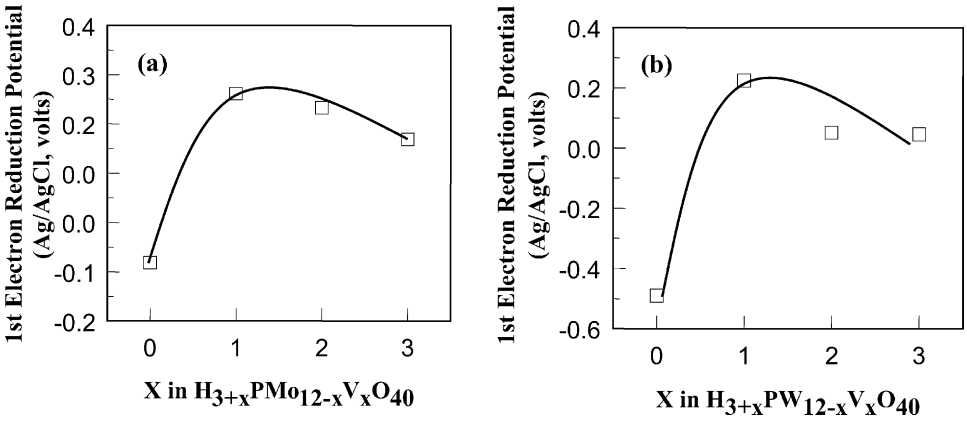

Fig. 8. Reduction potentials of polyatom-substituted HPAs as a function of vanadium content, established for (a) $H_{3+x}PMo_{12-x}V_xO_{40}$ ($x = 0, 1, 2, 3$) and (b) $H_{3+x}PW_{12-x}V_xO_{40}$ ($x = 0, 1, 2, 3$) HPAs.

metal centers and p-orbitals on the neighboring bridging oxygens [19]. Thus, substitution of vanadium ions into either the molybdenum or tungsten framework does not affect the energies of the HOMOs since they are almost entirely centered on the oxygens. However, the same substitution stabilized the LUMOs because these orbitals derive in part from vanadium d-orbitals which have been assumed to be more stable than those of molybdenum and tungsten. This implies that electrons added to the vanadium-substituted HPAs should be localized on the vanadium centers. Therefore, it is inferred that electrons added to the polyatom-substituted HPAs are localized on the less electronegative metal center. The less electronegative polyatom in the HPAs is much more efficient in the role of electron localization.

3.5. A map of reduction potential data of Keggin-type HPAs

Fig. 9 shows the map of reduction potential data established for all HPAs examined in this work, along with classification according to the exchange/substitution position. The tunability of reduction potential of HPAs depending on exchanged/substituted atoms and positions makes it possible for HPAs be chosen in a systematic way. The strong dependence of reduction potential of HPAs on electronegativity of the substituted atom and position makes it possible for us to predict or estimate the reduction potential of an HPA. The map of HPA reduction potentials can provide a design basis in searching for possible HPA candidates for selective oxidations.

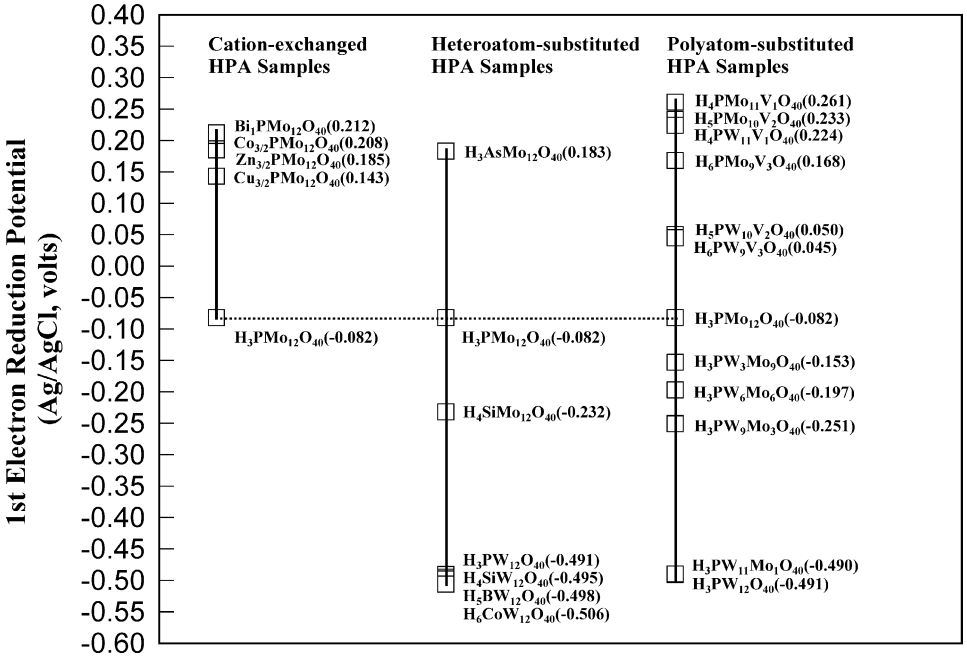

Fig. 9. A map of reduction potential data of Keggin-type HPAs determined electrochemically.

4. Conclusions

The measured reduction potentials of cation-exchanged, polyatom-substituted, and heteroatom-substituted HPA samples were correlated with the electronegativity of the substituted metal atom. The reduction potential measured for both cation-exchanged and heteroatom-substituted HPAs increased with increasing electronegativity of counter-cations or heteroatoms. However, the dependence of polyatom electronegativity on the reduction potential of polyatom-substituted HPAs was the opposite of those observed for cation-exchanged and for heteroatom-substituted HPAs; the reduction potential of polyatom-substituted HPAs increased with decreasing electronegativity of the substituted polyatom. A map of reduction potentials of HPA samples shows how one can vary the reduction potential of an HPA sample with electronegativity of the substituted metal atom.

Acknowledgements

This work was supported by the Korea Research Foundation Grant (KRF-2002-041-D00126).

References

[1] M.T. Pope, A. Müller (Eds.), Polyoxometalates: From Platonic Solids to Anti-retroviral Activity, Kluwer Academic Publishers, Dordrecht, The Netherlands, 1994.
[2] J.F. Keggin, Nature 131 (1933) 908.
[3] I.V. Kozhevnikov, Catal. Rev. -Sci. Eng. 37 (1995) 311.
[4] C.L. Hill, C.M. Prosser-McCartha, Coord. Chem. Rev. 143 (1995) 407.
[5] W.Y. Lee, I.K. Song, J.K. Lee, G.I. Park, S.S. Lim, Korean J. Chem. Eng. 14 (1997) 432.
[6] J.S. Choi, I.K. Song, W.Y. Lee, Korean J. Chem. Eng. 17 (2000) 280.
[7] G.I. Park, W.Y. Lee, I.K. Song, HWAHAK KONGHAK 38 (2000) 155.
[8] W.Y. Lee, I.K. Song, HWAHAK KONGHAK 38 (2000) 317.
[9] M.T. Pope, Heteropoly and Isopoly Oxometalates, Springer-Verlag, New York, 1983.
[10] M. Misono, Catal. Rev. -Sci. Eng. 29 (1987) 269.
[11] I.K. Song, S.H. Moon, W.Y. Lee, Korean J. Chem. Eng. 8 (1991) 33.
[12] H.C. Kim, S.H. Moon, W.Y. Lee, Chem. Lett. (1991) 447.
[13] N. Mizuno, M. Iwamoto, M. Tateishi, Appl. Catal. A 128 (1995) 1165.
[14] M.A. Barteau, J.E. Lyons, I.K. Song, J. Catal. 216 (2003) 236.
[15] I.K. Song, J.E. Lyons, M.A. Barteau, Catal. Today 81 (2003) 137.
[16] N. Mizuno, M. Tateishi, M. Iwamoto, J. Chem. Soc. Chem. Commun. (1994) 1411.
[17] N. Mizuno, D.-J. Suh, W. Han, T. Kudo, J. Mol. Catal. A 128 (1995) 309.
[18] K. Eguchi, T. Seiyama, N. Yamazoe, S. Katsuki, H. Taketa, J. Catal. 111 (1988) 336.
[19] R.S. Weber, J. Phys. Chem. 98 (1994) 2999.
[20] J. Melsheimer, S.S. Mahmoud, G. Mestl, R. Schlögl, Catal. Lett. 60 (1999) 103.
[21] M. Ai, Appl. Catal. 4 (1982) 245.
[22] M.S. Kaba, I.K. Song, M.A. Barteau, J. Phys. Chem. 100 (1996) 19577.
[23] M.S. Kaba, I.K. Song, M.A. Barteau, J. Vac. Sci. Technol. A 15 (1977) 1299.
[24] I.K. Song, M.S. Kaba, M.A. Barteau, W.Y. Lee, HWAHAK KONGHAK 35 (1997) 407.
[25] I.K. Song, M.S. Kaba, M.A. Barteau, W.Y. Lee, Catal. Today 44 (1998) 285.
[26] M. Kinne, M.A. Barteau, Surf. Sci. 447 (2000) 105.
[27] I.K. Song, M.A. Barteau, J. Mol. Catal. A 182–183 (2002) 185.
[28] I.K. Song, R.B. Shnitser, J.J. Cowan, C.L. Hill, M.A. Barteau, Inorg. Chem. 41 (2002) 1292.
[29] M.T. Pope, G.M. Varga Jr., Inorg. Chem. 5 (1966) 1249.
[30] J.J. Altenau, M.T. Pope, R.A. Prados, H. So, Inorg. Chem. 14 (1975) 417.
[31] T. Okuhara, N. Mizuno, M. Misono, Adv. Catal. 41 (1996) 113.
[32] M. Sadakane, E. Steckhan, Chem. Rev. 98 (1998) 219.
[33] N. Keita, L. Nadjo, Mater. Chem. Phys. 22 (1989) 77.
[34] I.V. Kozhevenikov, Catalysts for Fine Chemical Synthesis: 2. Catalysis by Polyoxometalates, Wiley, West Sussex, England, 2002.
[35] I.P. Alimarin, E.N. Dorokhova, L.P. Kazanskii, G.V. Prokhorova, Zh. Anal. Khim. 35 (1980) 2000.
[36] V.A. Grigoriev, C.L. Hill, I.A. Weinstock, J. Am. Chem. Soc. 122 (2000) 3544.
[37] R. Strandberg, Acta Chem. Scand. A 29 (1975) 359.
[38] G.M. Brown, N.R. Noe-Spirlet, W.R. Busing, H.A. Levy, Acta. Cryst. B 33 (1977) 1038.
[39] L. Lee, J.X. Wang, R.R. Adzic, I.K. Robinson, A.A. Gewirth, J. Am. Chem. Soc. 123 (2001) 8838.
[40] S. Himeno, T. Osakai, A. Saito, Bull. Chem. Soc. Jpn. 62 (1989) 1335.
[41] M.S. Kaba, I.K. Song, S.H. Wasfi, M.A. Barteau, J. Electrochem. Soc. 149 (2002) E117.
[42] D.L. Kepert, J.H. Kyle, J. Chem. Soc. Dalton. Trans. (1978) 137.
[43] C.C. Kircher, S.R. Crouch, Anal. Chem. 55 (1983) 242.
[44] L. Pettersson, I. Andersson, L.-O. Öhman, Inorg. Chem. 25 (1986) 4726.
[45] M.A. Schwegler, J.A. Peters, H. van Bekkum, J. Mol. Catal. 63 (1990) 343.
[46] G.B. McGarvey, J.B. Moffat, J. Mol. Catal. 69 (1991) 137.
[47] A. Jürgensen, J.B. Moffat, Catal. Lett. 34 (1995) 237.
[48] P. Courtin, Rev. Chim. Mineral. 8 (1971) 221.
[49] S.M. Kulikov, I.V. Kozhevnikov, Izv. Akad. Nauk SSSR, Ser. Khim. (1981) 498.
[50] M.T. Pope, A. Müller, Angew. Chem. Int. Ed. Engl. 30 (1991) 34.
[51] I.V. Kozhevnikov, O.A. Kholdeeva, Izv. Akad. Nauk SSSR, Ser. Khim. (1987) 528.
[52] Unpublished results.
[53] K. Tanaka, A. Ozami, J. Catal. 8 (1967) 1.
[54] H. Taketa, S. Katsuki, K. Eguchi, T. Seiyama, N. Yamazoe, J. Phys. Chem. 90 (1986) 2959.
[55] I.V. Kozhevnikov, Russ. Chem. Rev. 56 (1987) 811.
[56] M. Akimoto, H. Ikeda, A. Okabe, E. Echigoya, J. Catal. 89 (1984) 196.